We are IntechOpen,
the world's leading publisher of
Open Access books
Built by scientists, for scientists

6,900
Open access books available

185,000
International authors and editors

200M
Downloads

Our authors are among the

154
Countries delivered to

TOP 1%
most cited scientists

12.2%
Contributors from top 500 universities

CLARIVATE ANALYTICS
BOOK CITATION INDEX
INDEXED

WEB OF SCIENCE™

Selection of our books indexed in the Book Citation Index
in Web of Science™ Core Collection (BKCI)

Interested in publishing with us?
Contact book.department@intechopen.com

Numbers displayed above are based on latest data collected.
For more information visit www.intechopen.com

EMG Decomposition and Artefact Removal

Adriano O. Andrade, Alcimar B. Soares,
Slawomir J. Nasuto and Peter J. Kyberd

Additional information is available at the end of the chapter

1. Introduction

Traditionally, in clinical electromyography (EMG), neurophysiologists assess the state of the muscle by studying basic units of an EMG signal, which are referred to as motor unit action potentials (MUAPs). Information regarding the morphology and rate of occurrence of MUAPs is often used for diagnosis of neuromuscular disorders. In addition, recent studies have shown that the analysis of the energy content of MUAPs is a possible way for discriminating among normal, neurogenic, and myopathic MUAPs [38], illustrating, thus, the clinical value of the interpretation of MUAP information.

A common way of obtaining such information is by observing MUAP activities on an oscilloscope and listening to their audio characteristics over the speakers. When doing this, the researcher is implicitly performing a time and frequency analysis of MUAPs. However, the results of this analysis are dependent on the experience of the investigator and on his ability to extract relevant information from the visual and auditory analysis. Furthermore, this procedure is time-consuming and prone to error.

The drawbacks related to the procedure described above have motivated the use of computer-based techniques for extraction of MUAPs from EMG signals [3, 19, 22, 27, 29, 32, 40]. Such methods, also known as EMG decomposition techniques, aim at classifying MUAPs generated by a common source into the same group. The results of this classification may provide information regarding the orchestration of the neuromuscular system, and therefore of the state of the muscle. A similar problem, often referred to as spike sorting, is found in the study of neuronal activities [25]. In this case, neuronal action potentials from the same source are classified into a common group.

Originally, the investigation of MUAP activities belonged to needle electromyographic (NEMG) studies, mainly because surface electrodes may easily produce an integration of many potentials, which precludes accurate study of their individual form. However, some recent studies have shown that the use of surface electrodes may be successfully applied for

detection of MUAPs from superficial muscles [8]. This advancement has received widespread support among researchers and clinicians because of the ease of use, reduced risk of infection, and the greater number of motor unit action potential trains obtained compared to needle sensor techniques [47].

Currently, computer-based EMG has become an indispensable tool for investigations seeking to explain the state of the muscle. Different methodologies, ranging from simple quantitative measures to automatic systems that enable the assessment of neuromuscular disorders, have been developed [30]. Such tools are important for standardization of results and also they may reveal important features in the signals, which might be barely perceived from a manual analysis [35].

A typical system for extraction of MUAPs from EMG signals may require several stages of signal processing, for instance, signal detection and filtering (i.e., artefact removal) [45], feature extraction or selection [36], data clustering or classification [23]. Specific research may be carried out in each of these steps.

2. Strategies for EMG decomposition

One of the most rudimentary strategies for isolation of MUAPs belonging to a common group is by means of a thresholding scheme. The central idea of this technique is to use a voltage threshold trigger for detection of MUAPs that have similar height, which is represented by the amplitude of the highest peak of a MUAP. In this method the experimenter positions the recording electrode so that MUAPs of interest are maximally separated from the background activity (noise). MUAP activities are then measured with a hardware threshold trigger, which generates a pulse whenever the measured voltage crosses the threshold. Such pulses may be used for triggering data collection and further storage of MUAPs or their occurrence time in a computer. The main advantages of this method are that: (i) It is easy to apply since it requires minimal hardware and software; (ii) It is a good starting point for detection of the strongest MUAPs. The main drawbacks of this technique are that: (i) The threshold level, mainly dependent on the signal-to-noise ratio, determines the trade-off between missed spikes (false negatives) and the number of background events that cross the threshold (false positives); (ii) Only a single feature (the MUAP highest peak) is used for data classification. As a consequence of this strategy two MUAPs with different shapes might be grouped together because they have similar peak amplitude.

The drawbacks related to the technique discussed above highlight the importance of a pre-processing stage prior to grouping MUAPs. The presence of high levels of background activity in the signal suggests that the use of a filter for reduction of the background activity is necessary. Different digital filters may be used for this purpose. Typically high band-pass filters are used for attenuation of very low frequency components in the signal related to noise, which can be either inherent from the hardware used for data acquisition or the contribution of distant MUAPs from the detection point.

Another common approach is the use of differential filters. Such filters are low-pass filters and have been used in many investigations. The main drawback of such filters is that they may generate artificial spikes and modify the shape of MUAPs. This has motivated

the use of alternative filtering procedures, for instance, wavelets and a spatial filter, known as a Laplacian filter. The implementation of these filters as well as the introduction of an alternative method for EMG signal filtering is further discussed in the chapter.

Another relevant pre-processing step is the one that segments the EMG signal into windows containing active and inactive segments. This is a signal detection stage which aims to identify the activities of single MUAPs or their combinations, which is known as MUAP overlaps. Furthermore, this step separates noise in inactive segments from useful information in active segments. The detection of active and inactive segments may be performed visually or manually, i.e. the researcher may classify regions of an electromyographic signal into one of those categories, however such a method is time-consuming and requires concentration, which may introduce inconsistency in the signal analysis.

Different approaches may be employed for automation of this pre-processing stage: (i) The use of the root-mean square of the EMG signal together with a pre-defined threshold; (ii) A threshold proportional to the maximum peak in the signal; (iii) A threshold which is manually adjusted; (iv) Wavelets. The main assumption of this method is that there might be similarity between the mother wavelet and action potentials, and when the correlation between an active window and the mother wavelet is high an active segment is detected.

As one may note there exists a variety of strategies that could be considered for automation of the detection of active and inactive segments. Techniques that make an assumption about a pre-defined height and width of MUAPs may be more susceptible to failures, i.e. active regions that do not fit the predefined window will not be detected. Note also that the level of the background activity in the signal will also influence the determination of the beginning and end of active segments. The detection of active regions is further discussed in this chapter.

After detection of active regions it is possible to group them into logical units (clusters), however, it is very common to obtain features from those regions prior to data clustering. For example, morphological features of MUAPs, i.e. duration, amplitude, area, number of phases (number of baseline crossings) and number of turns (number of positive and negative peaks) have been employed. Other successful approaches include the use of coefficients of the Fourier transform, the coefficients of the Wavelet transform, the use of time samples of the band-pass filtered signal and low-pass differentiated signal, and the use of autoregressive and cepstral coefficients. Some other approaches, known as feature extraction and selection procedures, try to obtain features that maximize cluster separability. Examples of the use of such techniques include the application of Principal Component Analysis (PCA) and Independent Component Analysis (ICA).

The grouping of MUAPs is commonly performed by means of at least three distinct strategies: (i) Template matching: raw MUAPs, referred to as MUAP templates, are first classified or identified, and then used for classification of new MUAPs. The initial MUAP templates may be manually selected from the EMG signal or be chosen automatically from a clustering procedure. During data classification, usually MUAP templates are modified by an update rule, which takes into account the variability of MUAP shapes in the data set; (ii) Clustering: a clustering technique is used for grouping patterns represented by features selected from active regions; (iii) Hybrid: in this approach, first a clustering technique is used for grouping

part of the data set (normally the first 3 to 5 seconds), and then the non-classified data set is grouped into one of the classes defined in the first step.

Both the template matching and hybrid techniques require a priori identification of patterns in the data set before classification of the entire data set. The main disadvantage of these methods is that if new MUAP classes appear they will not be identified. The main advantage is that extra information regarding MUAP activities, e.g. the study of the firing time of MUAPs, may be taken into account in the final classification. The clustering approach has the advantage that it makes no assumptions about the data set to be grouped.

The main processing steps discussed so far form the basis of a complete EMG decomposition system. When the final application of such system is to study the firing behaviour of sources that generate MUAPs, it may be necessary to include an extra stage that deals with a problem known as MUAP overlaps. Overlapping spikes occur when two or more spikes fire simultaneously. When using the clustering technique for grouping active segments it may be possible to detect such overlaps as outliers. There are at least three strategies for dealing with overlaps: (i) Once a spike is classified it is subtracted from the active segment, in the hope that this will improve the classification of subsequent spikes. This approach requires a template of the spike. It yields reasonable results when two spikes are separated well enough so that the first can be accurately classified, but fails when the spikes are close together. Another problem with this approach is that the subtraction can introduce more noise into the waveform if the spike model (template) is not accurate. Also subtraction-based approaches may introduce spurious spike-like shapes if the spike occurrence is not accurately estimated; (ii) Another approach is to compare all possible combinations of two or more spike models. However, for some applications the computation time for performing this comparison may be prohibitive; (iii) The use of multiple electrodes or an array of electrodes may reduce the problem of overlapping spikes, because what appears as an overlap on one channel might be an isolated unit on another. Since the main aim of solving the overlapping problem is to increase the accuracy of estimators (e.g. mean) obtained from the firing of motor units, an alternative option might be to work directly with a precise estimate of the estimator considering missing data points (i.e that some MUAPs are missing).

Finally, once the system is designed and implemented it is important to test its accuracy. At least three methods are well accepted for this purpose: (i) Synthetic signals: artificial EMG signals are generated and employed for testing the stages of the system. The main advantage of this approach is that the characteristics of the analyzed signal are totally known; (ii) Manual classification of MUAPs: MUAPs are visually classified by the researcher and the results of this classification are used as reference for evaluation of the automatic classification; (iii) Comparison between MUAP activities from different channels: the consistency of the decomposition data of the same units from two different electrodes provides an indirect measure of the accuracy in real data decomposition.

3. Artefact removal from EMG signals

The detection of electromyographic signals is a very complex process, which is affected not only by the muscle anatomy and the physiological process responsible for the signal generation but also by external factors, for instance, the inherent noise of the hardware

employed in the signal amplification and digitalization. As a result EMG signals are often corrupted by noise.

It may be very difficult, if possible at all, to extract useful information from very poor signal-to-noise ratio EMG signals. In some applications, for example, the decomposition of electromyographic signals, a high level of background activity could impede the accurate segmentation of the signal into regions of activity that may represent the activity of single motor unit action potentials, influencing thus the final results of the EMG decomposition.

3.1. Conventional methods for EMG signal noise removal

3.1.1. Low-pass differential filter

Since its introduction, the low-pass differential filter (LPD) [44] has been widely employed in EMG signal processing [15, 19, 32, 40–42]. This filter is implemented in the time-domain as:

$$y_k = \sum_{n=1}^{N} (x_{k+n} - x_{k-n}),$$ (1)

where x_k is the discrete input time-series and y_k is the filtered output. N is the window width to adjust the cut-off frequency. Increasing N will reduce the cut-off frequency of the filter. This may be easily perceived if Equation 1 is studied in the frequency domain.

For this, consider the following difference equation obtained from Equation 1:

$$y[k] = \sum_{n=1}^{N} x[k+n] - \sum_{n=1}^{N} x[k-n].$$ (2)

Its representation in the frequency domain may be obtained via its Z transform as follows,

$$Z(y[k]) = Z\left(\sum_{n=1}^{N} x[k+n]\right) - Z\left(\sum_{n=1}^{N} x[k-n]\right)$$

$$Z(y[k]) = \sum_{n=1}^{N} Z(x[k+n]) - \sum_{n=1}^{N} Z(x[k-n])$$

$$Z(y[k]) = Y(z) = \sum_{n=1}^{N} z^n X(z) - \sum_{n=1}^{N} z^{-n} X(z)$$

$$Y(z) = X(z) \left(\sum_{n=1}^{N} (z^n - z^{-n})\right) \Bigg|_{z=e^{\frac{j2\pi f}{f_{sr}}}}$$

where the ratio $Y(z)/X(z)$ is the filter transfer function $H(z)$, f is the frequency in Hz and f_{sr} is the sampling frequency in Hz.

Figure 1 presents the results of the estimate of the filter transfer function with different sizes of windows, $N = 40$ and $N = 20$. Note how the cut-off frequency is shifted to a higher frequency when the window size is reduced.
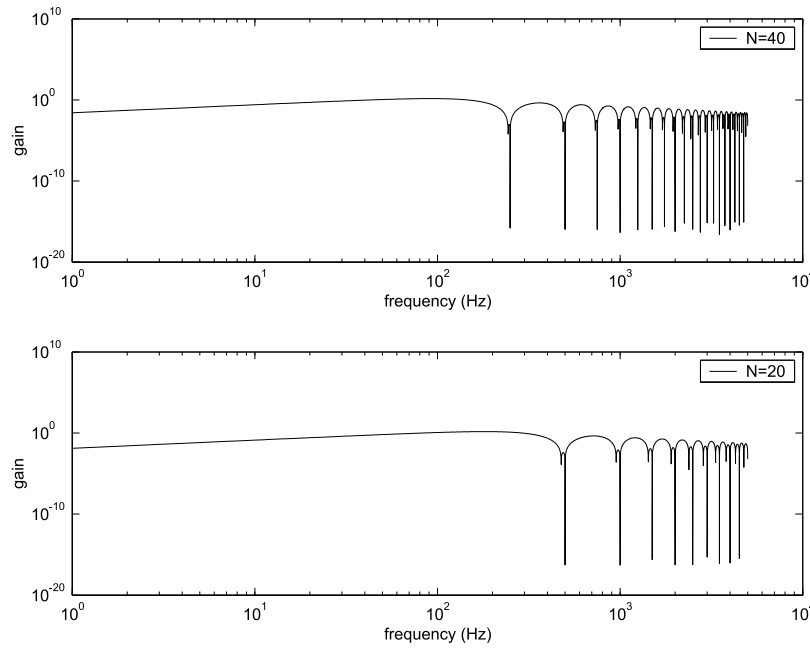
Figure 1. Frequency response of an LPD filter with window width 20 and 40.

The main advantages of using the LPD filter are that it is very easy to implement, and it is considerably fast for real-time applications, but some drawbacks regarding this filter are discussed in [46]:

- Under conditions of low signal-to-noise ratio the relatively strong high frequency noise (background activity) may be accentuated;
- Since the LPD filter is not an ideal low-pass filter, there will exist severe Gibbs phenomenon, that is, the leakage of energy frequency out of the filter pass-band as illustrated in the Bode diagrams shown in Figure 1. As a result, many high frequency noise components will pass through the filter.

3.1.2. Weighted low-pass differential filter

The weighted low-pass differential filter (WLPD) was proposed in [46] as an alternative to the LPD filter. The main difference is that an appropriately weighted window is included in Equation 2 for reduction of the Gibbs effect. The WLPD filter is implemented in the time-domain as:

$$y_k = \sum_{n=1}^{N} w(n)(x_{k+n} - x_{k-n}), \tag{3}$$

where $w(n)$ is an N point windowing function. Several windows such as Barlett, Hamming and Hanning may be employed. If a rectangular window is used then Equation 3 is an LPD filter. Similarly to the LPD filter the WLPD is very easy to implement and considerably fast for real-time applications, but results presented in [17, 46] show that phase distortion may
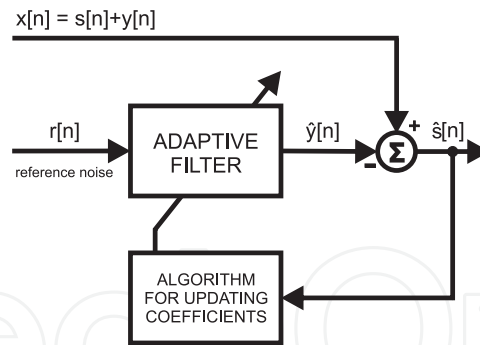
Figure 2. Adaptive noise canceller. $x[n]$ is the noise corrupted signal, $s[n]$ is the noise free signal, $y[n]$ the noise and $r[n]$ the reference noise. $\hat{y}[n]$ is the estimated noise, whereas $\hat{s}[n]$ the estimated signal.
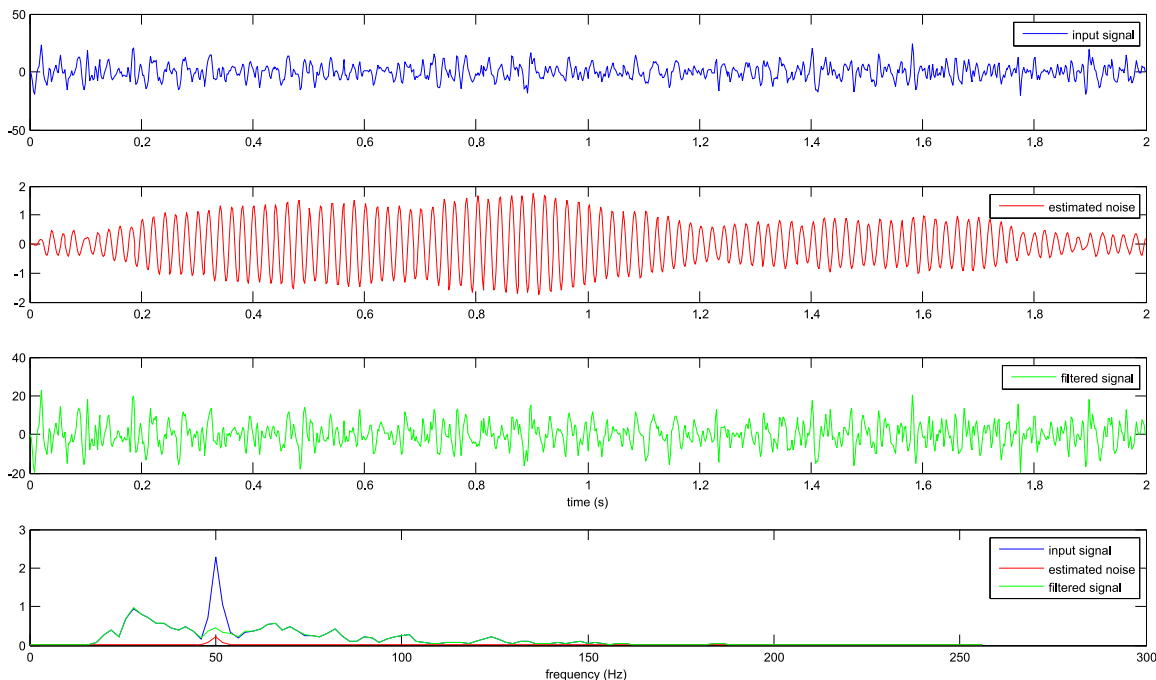

Figure 3. Example of application of the adaptive noise cancelling on a sample of EMG signal. The corrupted signal (top) is contrasted with the cleaned signal. The power spectra of the signals are shown at the bottom and illustrate the effect of the application of the filter on the 50 Hz component.

be present in the filtered signal and depending on the level of noise false spikes may be generated.

3.1.3. Adaptive 50/60 Hz noise cancellation

When the source of noise is well known it is possible to employ methods for adaptively reduce its influence over the desired signal. This is, for instance, the aim of adaptive 50/60 Hz noise cancellation based on the least mean square (LMS) algorithm [2].

The block diagram shown in Figure 2 depicts the main idea of the adaptive noise cancelling algorithm. The signal $s[n]$ is corrupted by the noise $y[n]$ yielding the corrupted signal $x[n]$. The adaptive algorithm will estimate parameters for a filter capable of attenuating the desired

components and maintaining relevant information from the signal. The piece of code below is a Matlab function created for attenuating 50 Hz noise from signals. It was used to illustrate the application of the technique on an EMG signal which was strongly corrupted by 50 Hz noise. The plots given in Figure 3 show the input signal, the estimated noise and the filtered signal. The power spectra of these signals are given in the graph at the bottom. Their analysis allows us to conclude that the application of the adaptive filter attenuated the undesired 50 Hz component. Note that the 50 Hz component is also part of the EMG signal, therefore its complete elimination is not desired.

```
function [EstimatedNoise,filteredSig50Hz] = NoiseRemoval(x,fs)
%% Function name....: NoiseRemoval
% Description......:
%                    This function estimates a filtered signal based on a
%                    50Hz noise optimal filter (LMS algorithm)
% Parameters.......:
%                    x ......-> input time-series
%                    fs......-> sampling frequency (Hz)
% Return...........:
%                    EstimatedNoise... -> estimated 50 Hz noise
%                    filteredSig50Hz.. -> filtered signal (50 Hz noise free signal)

mu = 0.001; %constant of convergence of the LMS algorithm
taps = 10; %filter order
t = [0:1:length(x)-1]/fs;
d  = sin(2*pi*t*50);  % reference noise (component to be removed from the input signal)
ha = adaptfilt.lms(taps,mu);
[y,e] = filter(ha,d,y);
[EstimatedNoise,filteredSig50Hz] = filter(ha,d,e);
```

3.1.4. Signal filtering based on wavelets

One of the main applications of wavelets is noise removal from corrupted signals. A general procedure for signal de-noising involves the following three steps that have been successfully applied [14, 16, 33]:

1. Signal decomposition;
2. Detail coefficients thresholding;
3. Signal reconstruction.

In the first step, both a wavelet prototype and the decomposition level (N) are chosen, and the wavelet decomposition of the signal at level N is performed. In the next step, for each level from 1 to N, a threshold, t_N, is selected and soft-thresholding is applied to detail coefficients as shown in Equation 4.

$$Y_N = sign(D_N)(|D_N| - t_N)_+ \tag{4}$$

where Y_N is the de-noised version of the Nth detail coefficients and the function $(x)_+$ is defined as

$$(x)_+ = \begin{cases} 0, & x < 0 \\ x, & x >= 0. \end{cases} \tag{5}$$

Finally, in the third step the denoised signal is estimated by using the original approximation coefficients of level N and the modified detail coefficients of levels from 1 to N. The application of this procedure is illustrated in the following example.

3.1.5. Example of application

The procedure for noise removal based on wavelets is applied to an experimental surface EMG signal in this section. The main aim is to attenuate the background activity present in the signal and at the same time to preserve its shape.

The Matlab Wavelet Toolbox[1] is used for data processing (see Figure 4). The EMG signal is decomposed into three levels ($N = 5$) and the $db5$ wavelet prototype is employed. The choice for the decomposition level may be justified by the fact that this signal is mostly contaminated by high frequency noise that will be highlighted by short time-scale components (e.g. detail coefficients of the first and second level) and therefore further decomposition would not contribute significantly to the final form of the filtered signal. The criteria for selection of the wavelet family (Daubechies) is mainly because of its reported success in removing/attenuating noise from EMG signals, and in its use for feature extraction from MUAPs [18, 37, 48].

The results of the signal decomposition are depicted in Figure 4. A window of the input EMG signal together with its filtered version are presented in Figure 5.

3.2. EMG signal filtering based on Empirical Mode Decomposition

In this section a novel algorithm for signal de-noising based on the Empirical Mode Decomposition (EMD) method is presented [7]. The developed filter may be employed as an alternative to the approach based on wavelets described above.

3.2.1. The Empirical Mode Decomposition method

Huang *et al.* (1998) [21] described a new technique for analyzing nonlinear and non-stationary data. The key part of the method is the Empirical Mode Decomposition (EMD) method, in which any complicated data set can be adaptively decomposed into a finite, and often small, number of Intrinsic Mode Functions (IMFs). The name Intrinsic Mode Function is adopted because those components represent the oscillation modes embedded in the data. In the case of Fourier analysis, oscillation modes (i.e. components) in a signal are defined in terms of sine and cosine waves. The EMD thus defines oscillation modes in terms of IMFs, which are functions that satisfy two conditions [21]:

1. In the whole time-series, the number of extrema and the number of zero crossings must be either equal or differ at most by one. Note that extrema are either local minima or local maxima. Furthermore, a sample g_i in a time-series is a local maximum if $g_i > g_{i-1}$ and $g_i > g_{i+1}$, and a sample q_i is a local minimum if $q_i < q_{i-1}$ and $q_i < q_{i+1}$, where i is a discrete time.

---

[1] This toolbox can be invoked by typing *wavemenu* in the Matlab command environment.
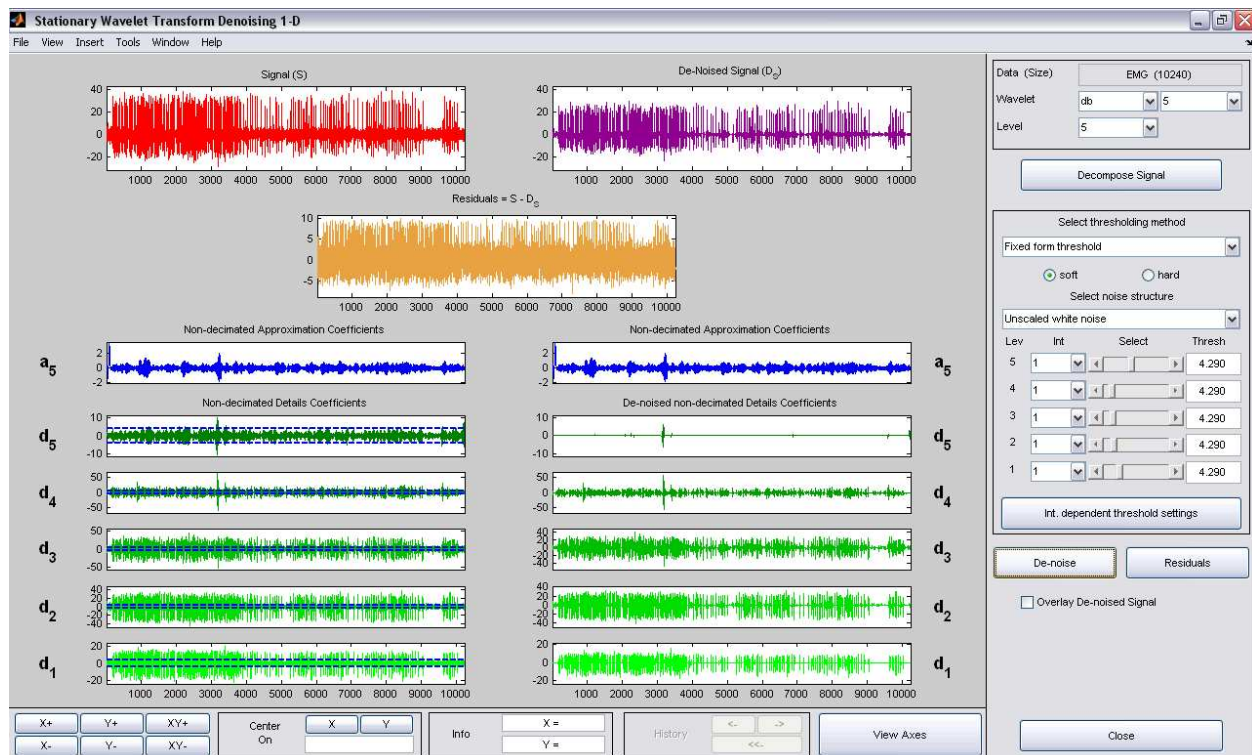
Figure 4. Graphical user interface of the Wavelet Matlab Toolbox used for signal denoising. The EMG signal and its denoised version are shown. The wavelet components are individually denoised by using a thresholding scheme.

2. At any point in the time-series, the mean value of the envelopes, one defined by the local maxima (upper envelope) and the other by the local minima (lower envelope), is zero.

The definition above is empirical and currently there is no explicit equation for estimating IMFs, thus any arbitrary time-series that satisfies conditions 1 and 2 is an IMF. Furthermore, by means of the analysis of the power spectra of IMFs it is possible to verify that these functions represent the original signal decomposed into different time-scales (or frequency bandwidths). This is illustrated in [4, 6]. Thus, both wavelets and the Empirical Mode Decomposition provide the decomposition of a signal into different time-scales. The main difference is that one method performs the signal decomposition adaptively and based solely on the available data, whereas the other normally uses a set of pre-fixed filters.

3.2.2. The algorithm for signal filtering based on the EMD

The success of the general procedure for noise removal using wavelets is based on the fact that it is possible to filter signal components individually instead of filtering the original signal. This is desirable because some components may highlight the noise and thus it may be easier to attenuate its presence.

Similarly, the Empirical Mode Decomposition also provides the decomposition of a signal into different time-scales or IMFs. This means that it is also possible to filter signal components individually instead of the original signal. This suggests that the strategy for signal de-noising
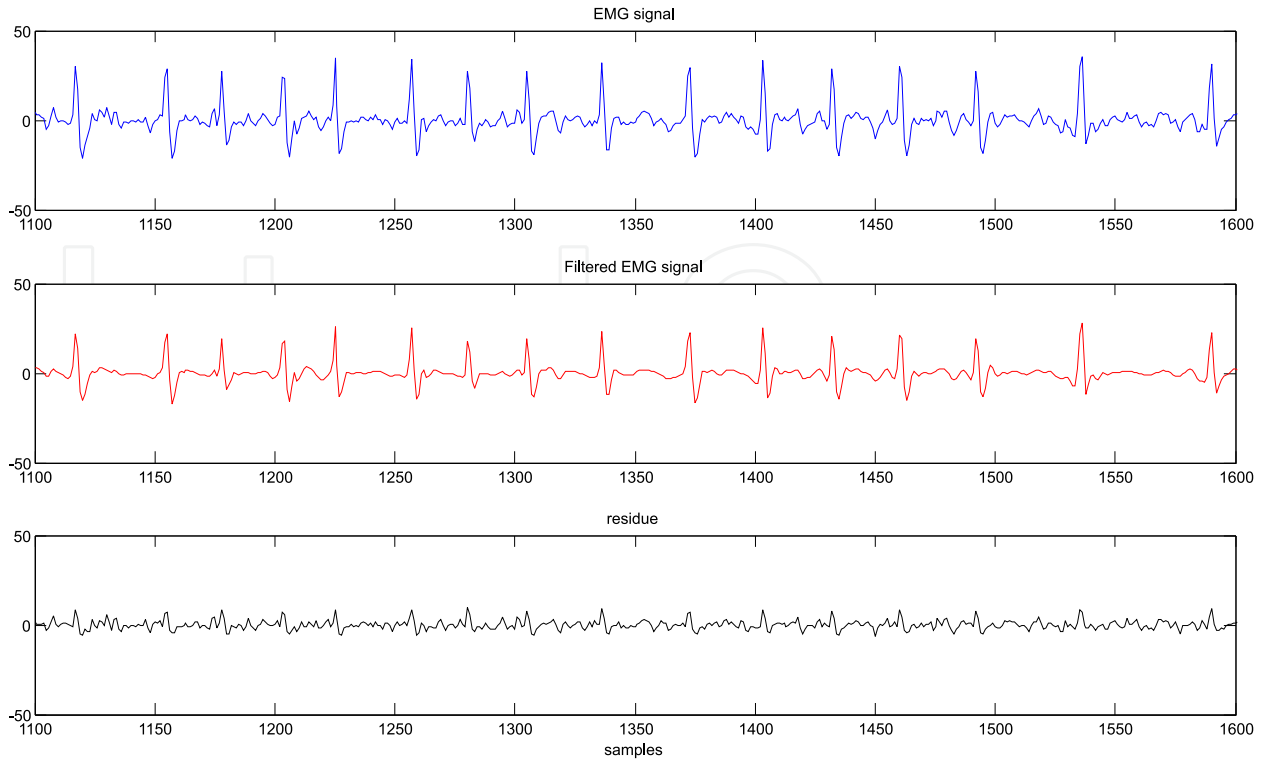
Figure 5. Segment of the EMG signal shown in Figure 4. The filtered signal and the residue is also presented.

based on wavelets may also be applied to intrinsic mode functions. Thus the following procedure was proposed for EMG signal filtering [3, 7]:

1. Decompose the signal into IMFs;
2. Threshold the estimated IMFs;
3. Reconstruct the signal.

This procedure is practical, mainly due to the empirical nature of the EMD method, and it may be applied to any signal as the EMD does not make any assumption about the input time-series. A block diagram describing the steps for its application is shown in Figure 6. First, the EMD method is used for decomposing the input signal into intrinsic mode functions, $IMF_1, \ldots, IMF_N$, where N is the number of IMFs. These IMFs are then soft-thresholded, yielding $tIMF_1, \ldots, tIMF_N$, which are thresholded versions of the original components. The filtered signal is obtained as a linear summation of thresholded IMFs.

A very common strategy used in the filtering procedure based on wavelets is to use the soft-thresholding technique described in [14]. The same idea is used for thresholding IMFs. For each IMF from 1 to N a threshold, $t_n, n = 1, \ldots, N$, is selected and soft-thresholding is applied to individual IMFs.

The threshold t_n is estimated by using the following strategy: a window of noise is selected from the original signal and then the boundaries of this window are used to extract regions of noise from IMFs. The standard deviation of each of those regions is then estimated, and
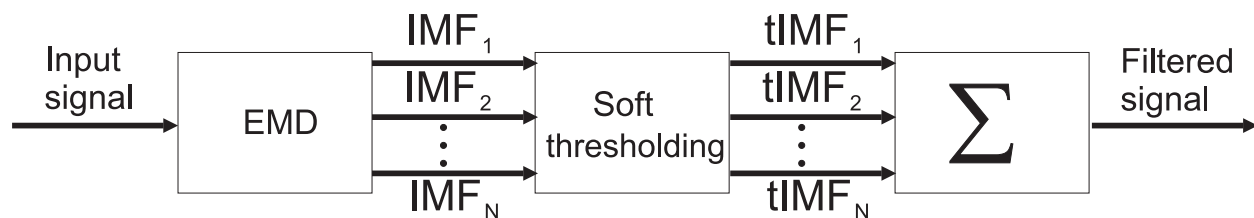
Figure 6. The EMD method is employed for decomposing the input signal into IMFs ($IMF_1, \ldots, IMF_N$, where N is the number of IMFs). These IMFs are soft-thresholded, yielding $tIMF_1, \ldots, tIMF_N$, which are thresholded versions of the original components. The filtered signal is obtained as a linear summation of thresholded IMFs.
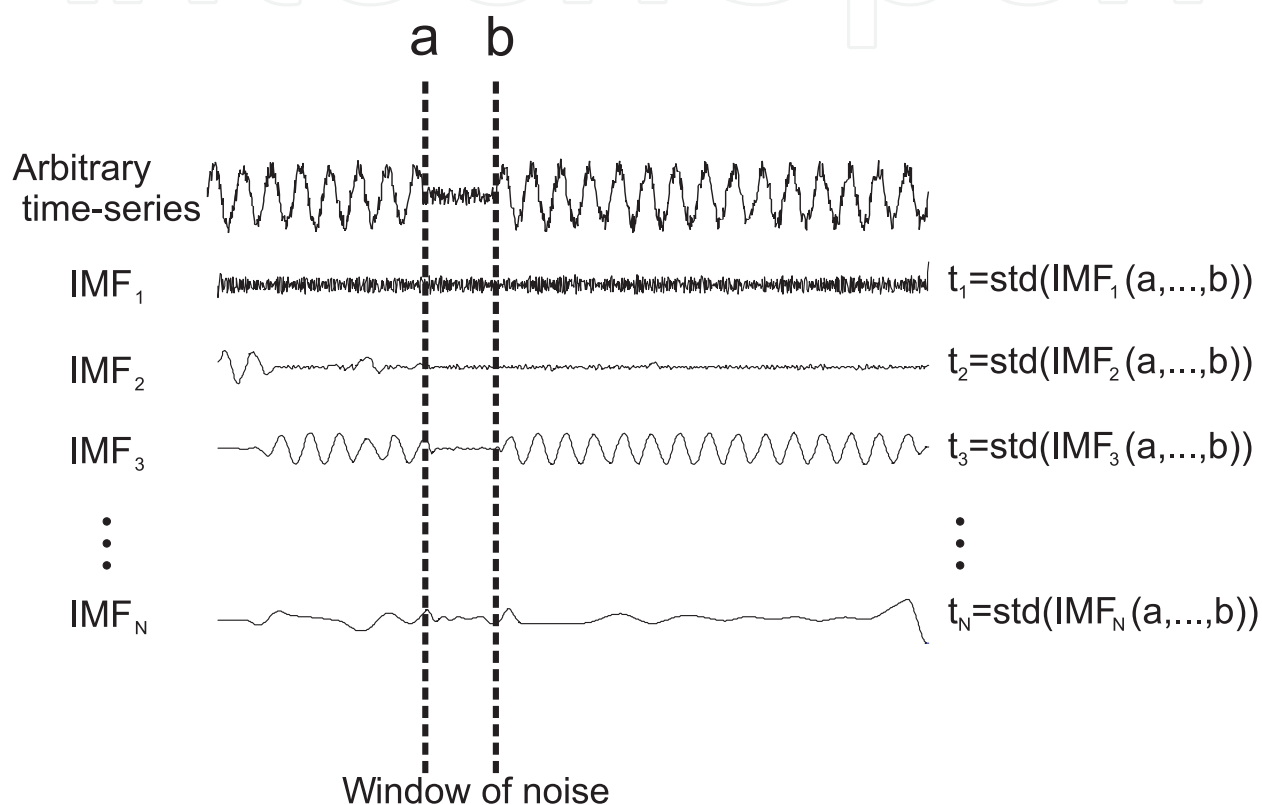

Figure 7. Illustrative example showing the estimate of thresholds t_n. First, a window of noise (i.e. samples within the interval [a,b]) is selected from the arbitrary time-series. The interval [a,b] is employed for selection of noise in the IMFs, and then from each IMF, thresholds $t_1, \ldots, t_N$ are defined. Note that *std* is the standard deviation.

these are regarded as the required thresholds ($t_1, \ldots, t_N$). Figure 7 illustrates the procedure for estimating t_n.

3.2.3. An example of application of the filter based on the EMD method

In this section, an example illustrating the application of the procedure for filtering EMG signals based on the EMD is provided. For this, the experimental surface electromyographic signal shown in Figure 8 is used.
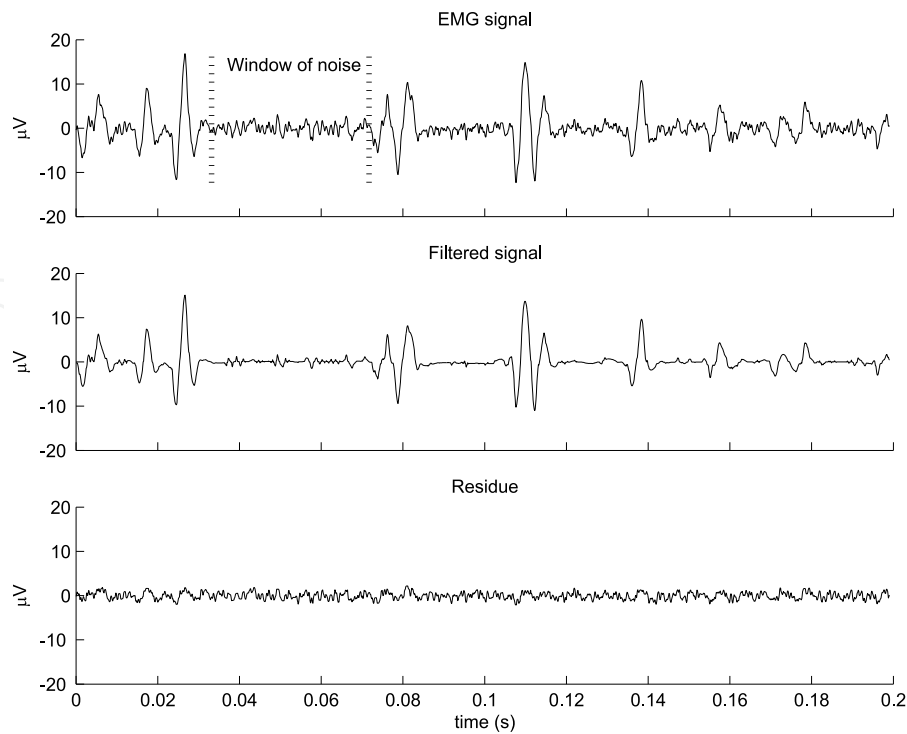
Figure 8. EMG signal and its filtered version. The residue, which is the difference between those signals is also shown.

The first step of the algorithm is to use the EMD (or sifting process) to decompose the experimental signal into intrinsic mode functions. Eight IMFs ($IMF1, \ldots, IMF8$) are obtained and they are presented in Figure 9(a).

The subsequent step is to threshold the components $IMF1, \ldots, IMF8$. Equation 4 was employed for denoising individual IMFs. The results of this procedure are shown in Figure 9(b). Note that in order to estimate thresholds for IMFs the boundaries of the window of noise (0.03 s and 0.07 s) indicated in Figure 8 were selected.

In the last step, the resulting (de-noised) components were combined to generate a filtered version of the original signal as shown in Figure 8. In the same figure, the residue, which is the difference between the original and filtered signals, is also presented. The random nature of this component and the attenuation of the noise in the EMG signal is apparent.

4. A system for extraction and visualization of MUAPs

The visual inspection of data is an important stage in signal analysis. It may help the investigator to identify relevant features, outliers and noise in the signal. Although visualization is an important and basic stage in data processing, in practice, its execution may be rather complex, specially when performed manually and the data lie in a high dimensional manifold.

In this context tools or systems that allow for an automatic visualization of signals play an important role. First, they significantly reduce the overall processing time of data, and
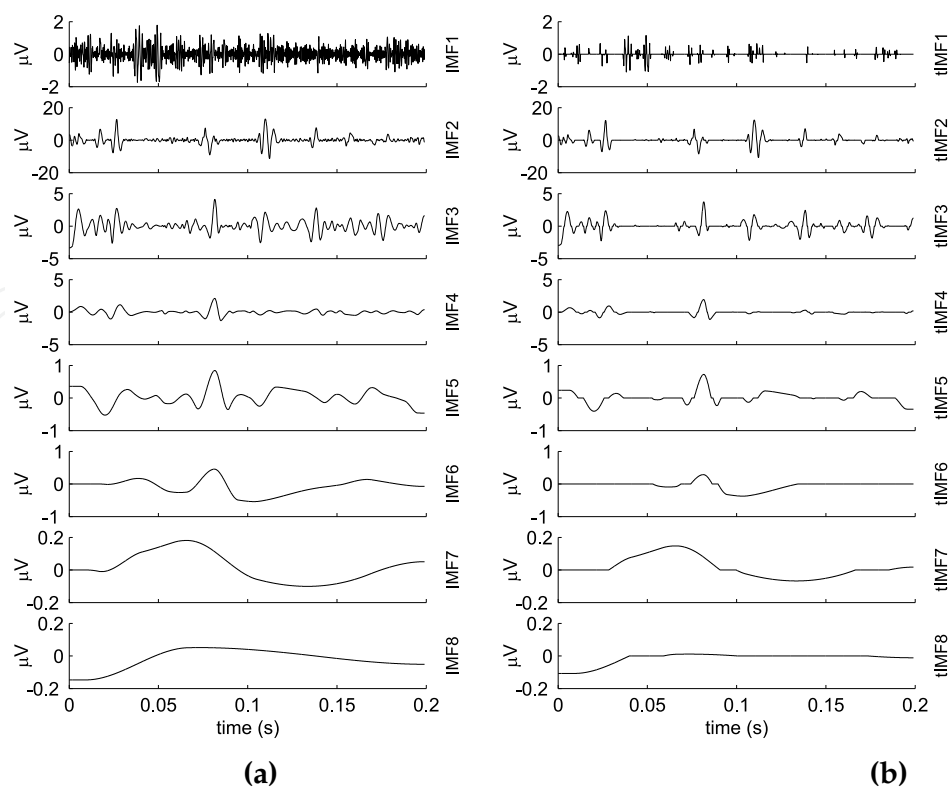
Figure 9. (a) Intrinsic mode functions ($IMF1, \ldots, IMF8$) obtained from the EMG signal presented in Figure 8. (b) De-noised intrinsic mode functions.
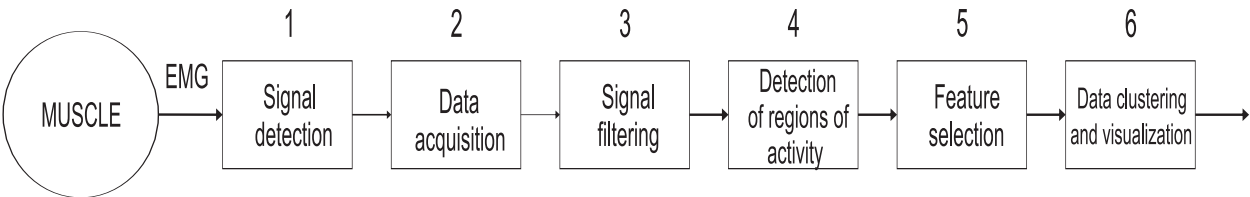

Figure 10. Block diagram of the system for extraction and visualization of MUAPs. After detection (1) and acquisition (2) the EMG signal is filtered (3), and signal windows, designated as regions of activity (RA), are extracted from it (4). In (5) features are selected from RA and then employed for their clustering and visualization.

secondly they may reveal information present in the signal which might be barely perceived in a manual analysis.

This section describes a system that can be used for the extraction and visualization of motor unit action potentials from electromyographic signals. It is formed by several basic units which are illustrated in Figure 10. Its input is a raw electromyographic signal, and its output is the visualization of MUAPs or any other information (e.g. noise) present in the signal grouped into logical units (clusters). This visualization allows the researcher to identify outliers, noise and groups of MUAPs. Each of the stages of this system is described below.

Once the EMG signal is detected it is amplified and digitized. An EMG amplifier[2] and data acquisition board[3] are important elements that contribute to the correct collection of data.

---

[2] Typical requirements of the signal conditioner are CMRR > 80 dB, input impedance > 10^{15} Ω, noise level < 1.2 μV.

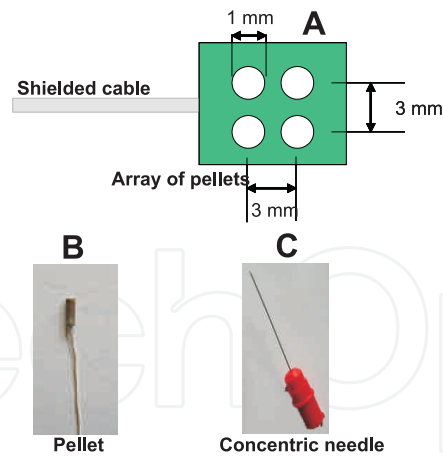[3] A possible model would be PC-card DAS 16/16 Measurement Computing

Figure 11. Types of electrodes for EMG signal detection. (A) A customized array of pellet electrodes. (B) Example of a single pellet electrode. (C) Concentric needle electrode.

Other relevant units include force sensors for monitoring the level of muscle contraction and biofeedback systems that provide a stimulus and information for subjects about the required task to be executed during the experiment.

4.1. System description

4.1.1. Signal detection and acquisition

The stage of signal detection will convert current generated by movement of ions (a physiological process) into current generated by movement of electrons (an electrical process). The choice of the type of electrode to be employed is dependent on the aim of the investigation. For instance, if the interest is to extract and visualize activity of motor unit action potentials from EMG signals, then needle electrodes are traditionally employed, mainly because of the high spatial resolution offered by these sensors. In fact, when studying the state of deep muscles this is the only possible choice. However, many studies [5, 11, 17, 43, 49] have shown that surface EMG electrodes with a sufficiently small contact surface may be successfully applied to the detection of MUAP activity in superficial muscles.

The system depicted in Figure 10 has been tested with two types of electrodes for signal detection. They are shown in Figure 11. One is a concentric needle electrode and the other is a customized array of pellet(surface) electrodes whose dimensions follow specifications provided in [43]. Both electrodes are passive and leads connecting them to the amplifier are shielded in order to attenuate the presence of spurious noise activity.

The use of pellet electrodes was a very cheap and simple solution for high spatial resolution signal detection, which yielded outstanding results and consistent detection of EMG signals.

4.1.2. Signal filtering

The main aim of this stage is to reduce the background activity present in electromyographic signals. This is relevant because high levels of background activity (noise) may affect the
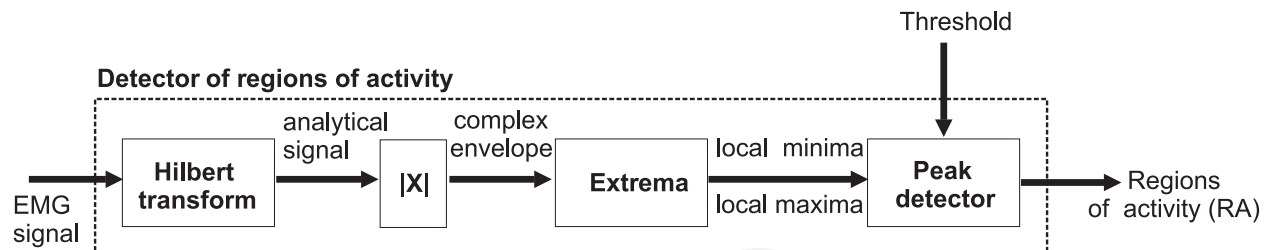
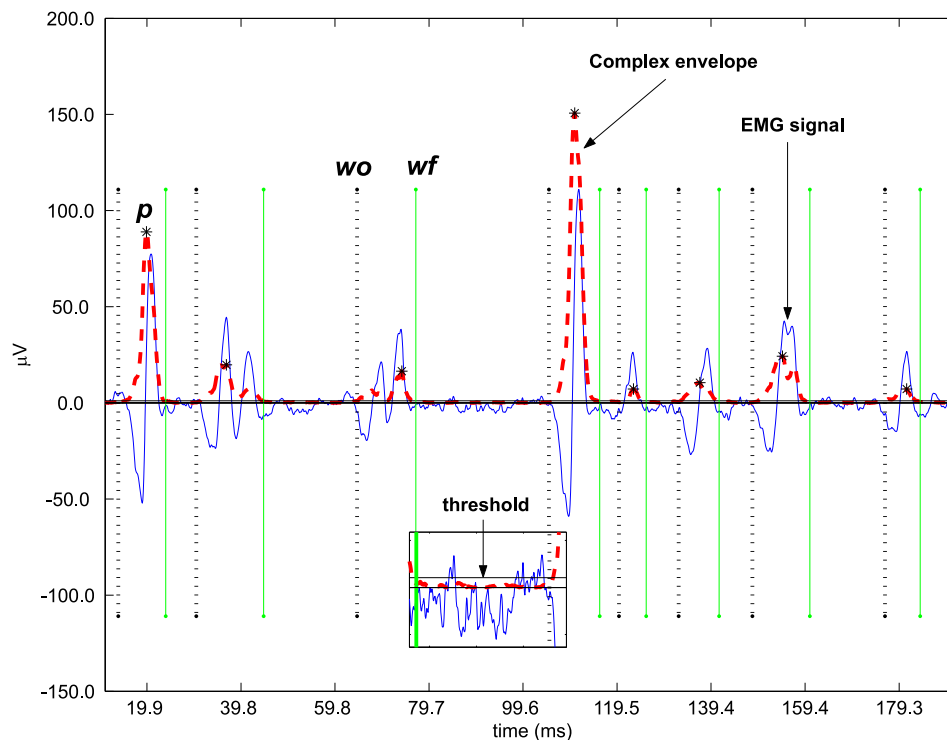**Figure 12.** Block diagram of the detector of regions of activity.

Figure 13. Example of detection of regions of activity. The experimental surface EMG signal and its complex envelope are shown. w_o and w_f are respectively the beginning and end of a region of activity. The peak (p) within each RA is marked with $*$ and it is used as a reference point for feature selection. The inset shows a window of noise with the pre-defined threshold level.

detection of useful information (e.g. MUAPs). This stage may be performed by the filtering procedure based on the Empirical Mode Decomposition described above.

4.1.3. Detection of regions of activity

Following the stage of signal filtering the EMG signal is segmented into small windows, so-called regions of activity (RA), that may contain the activity of single MUAPs, MUAP overlaps or noise. A detector of RA was devised for extraction of RA from EMG signals. The block diagram of this is shown in Figure 12 and an example of its application is provided in Figure 13. Its input may be either a raw or filtered EMG signal and the output is a set of regions of activity.

Basically, this system will estimate the signal envelope and it will select from it reference points which define the beginnings and ends of RAs. Intuitively, the envelope is the overall shape of the amplitude of the signal and its use instead of the raw signal may simplify, in terms of practical implementation, the solution for this problem, mainly because the signal envelope is positive. For instance, a unique positive threshold may be employed for selection of RAs which are above it.

The envelope of time domain signals can be computed by low pass filtering and curve fitting techniques [21], or by using the Hilbert transform to compute the analytic signal [13]. The signal envelope generated from the first two methods is dependent on the choice of parameters like the filter order and the method for data fitting, whereas in the latter strategy no a priori parameters should be set before calculation of the signal envelope. For this reason this is the method implemented in this system, that is, the absolute value of the complex analytic signal (also known as the complex envelope [13]) is used to estimate the signal envelope.

From the signal envelope, local minima and local maxima points are estimated. This will reduce the number of candidate points to be searched by the peak detector. As a consequence, the processing time will also be reduced, which may be relevant for the analysis of either long or oversampled time-series. Another benefit of this stage is that noise activity may be eliminated.

The role of the peak detector is to search for extrema points which are above or below a threshold. Once a maximum (w_o) is found, the mean of the small window, $h_o = w_o + u$, is estimated and only if this mean is above the pre-defined threshold, w_o will be selected as the beginning of an RA. In this system u is set to 1 ms. Note that the analysis of the mean of h_o may avert the selection of spurious activity (e.g. noise). The end of an RA is detected when a minimum (w_f) is found. In this case, w_f is considered to be valid only if the mean of the window $h_o = w_o - u$ is below the threshold.

The threshold, th, is estimated as $th = k \times std(W_{noise})$, where W_{noise} is a window of noise directly selected from the analysed signal, $std(W_{noise})$ is the standard deviation of W_{noise}, and k is a user-defined constant which controls the threshold level. A typical value for k is 5. It is supported by the Chebyshev theorem [26]. This theorem states that, for any distribution, if $k > 1$ then the fraction of observations that fall within a range of $\pm k \times std(W_{noise})$ around the mean is at least $F = 1 - (1/k^2)$. For instance, $F = 0.96$ for $k = 5$, which means in practice that any sample within the interval $[mean(W_{noise}) - k \times std(W_{noise}), mean(W_{noise}) + k \times std(W_{noise})]$ has a 96% chance of really being noise.

4.1.4. Feature selection

In the feature selection stage, features will be selected for use in data clustering from a window within the region of activity. Figure 14 shows reference points in time (w_o, p_o, p, p_f, w_f) for definition of this window.

w_o and w_f are respectively the time when the region of activity starts and ends. These points are estimated by the detector of regions of activity. p is the time when the highest peak in the
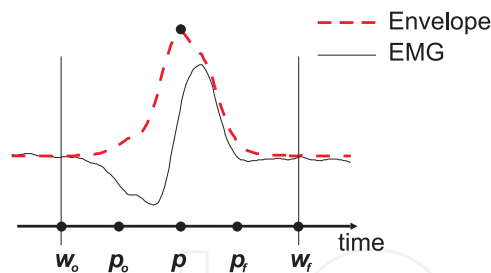
Figure 14. Identification of reference points in time for feature selection. w_o and w_f indicate the beginning and end of the region of activity. p is the time when the highest peak in the envelope and within the interval $[w_o, w_f]$ occurs, and p_o and p_f define the boundaries of a rectangular window for feature selection.

envelope of the RA occurs. This point is also the point where the variation in amplitude of the signal is maximal within the RA. This is illustrated in Figure 13.

p_o and p_f are respectively the beginning and end of the window to be selected for analysis. These points are defined as follows: $p_o = p - min\{t_o, p - w_o\}$ and $p_f = p + min\{t_o, w_f - p\}$, with t_o set to 2 ms. Note that the width of the window defined by p_o and p_f may vary for different RAs. Therefore, interpolation (splines) was employed for selection of 40 samples from each window defined in the interval $[p_o, p_f]$. This means that after feature selection each pattern is represented by a 40D vector with samples obtained via an interpolation procedure.

4.1.5. Data visualization and clustering

In order to ease the application of the sequence of steps detailed in Figure 10 a graphical user interface (GUI) was devised. The main GUI is shown in Figure 15. The system is capable of importing EMG data organized in columns of a text file and storing them in user-defined variables which are available in a list box. The main interface is organized into four logical sections (tabs) that should be accessed sequentially.

Figure 16 shows the module which allows the user to filter the EMG signal. The filtering procedure based on the Empirical Mode Decomposition is available here. The result of the automatic detection of regions activity is given in the interface shown in Figure 17.

The results of the data clustering and visualization step are presented in the GUI shown in Figure 18. At this stage patterns are clustered by means of Generative Topographic Mapping (GTM) and data visualization is performed with the GTM grid [3, 9]. For generation of the GTM grid, a GTM model with 25 Gaussian functions and 16 basis functions with a width of 1 is fitted to the data. The data can also be projected onto the two-dimensional space so that the user can visualize the distances of distinct groups of MUAPs (see Figure 19).

5. The application of EMG decomposition in the treatment of neuromuscular disorders triggered by stroke

Stroke, or cerebrovascular accident (CVA), affects a great number of individuals, and is the leading cause of disability among adults [10, 24]. After the event, most individuals must deal with severe reduction of motor functionality [31].
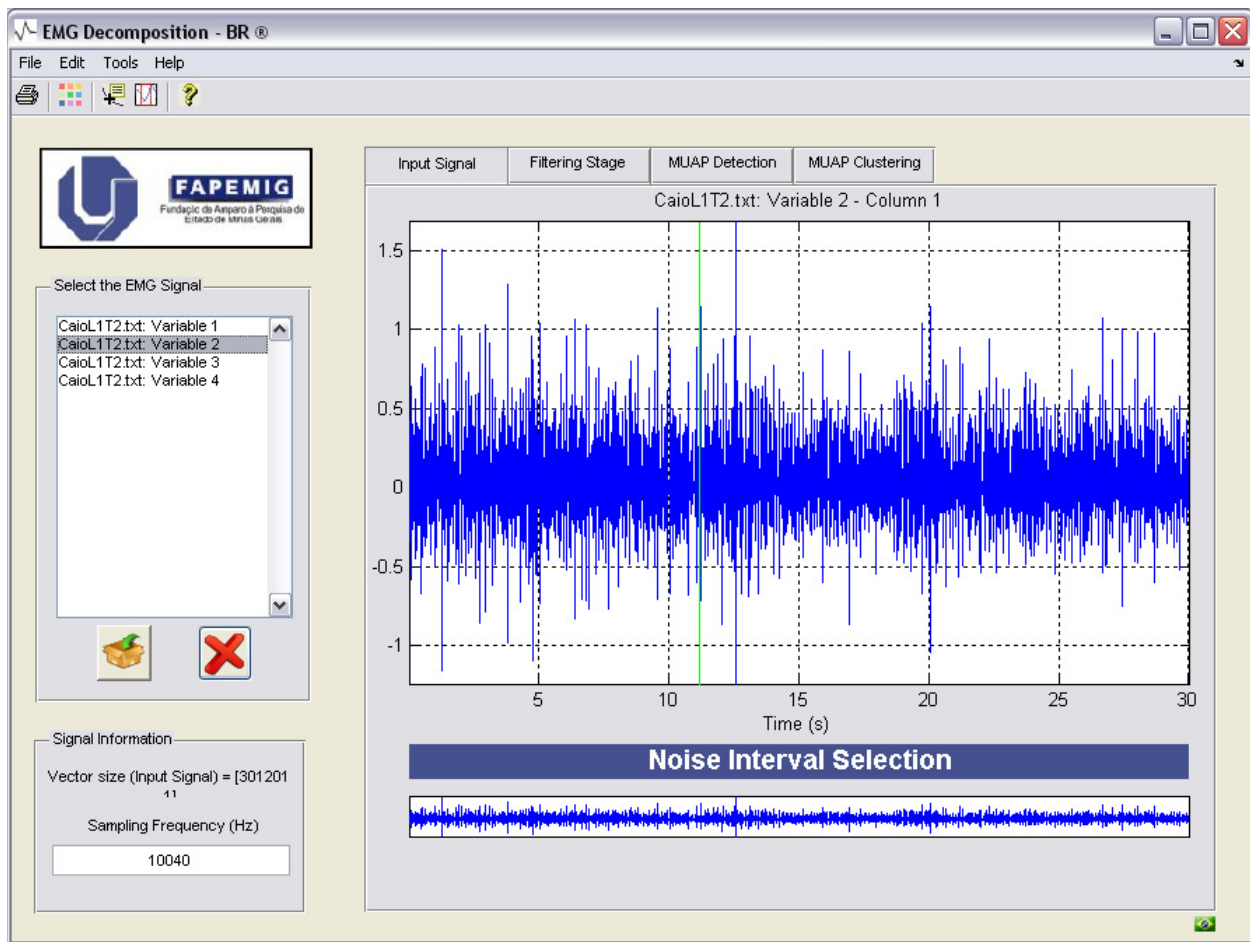
Figure 15. Main graphical user interface of a software that implements the sequence of steps detailed in Figure 10.
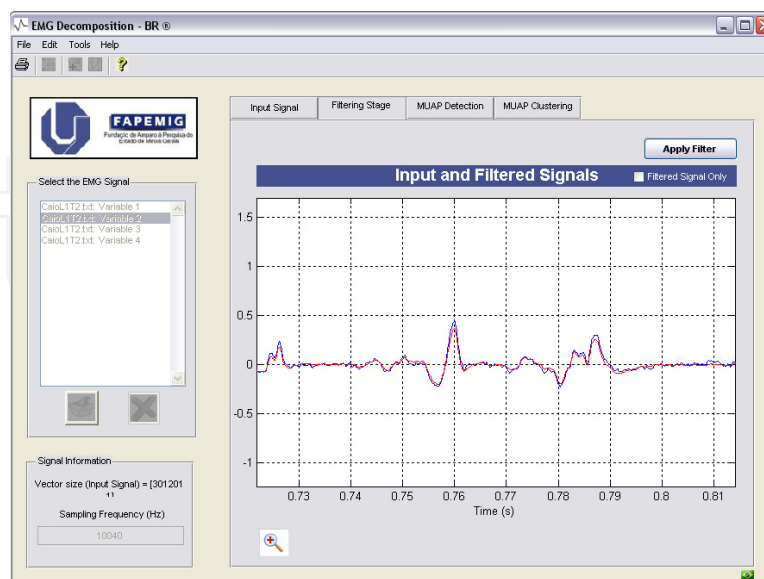

Figure 16. Graphical user interface which allows the user to filter the input signal.
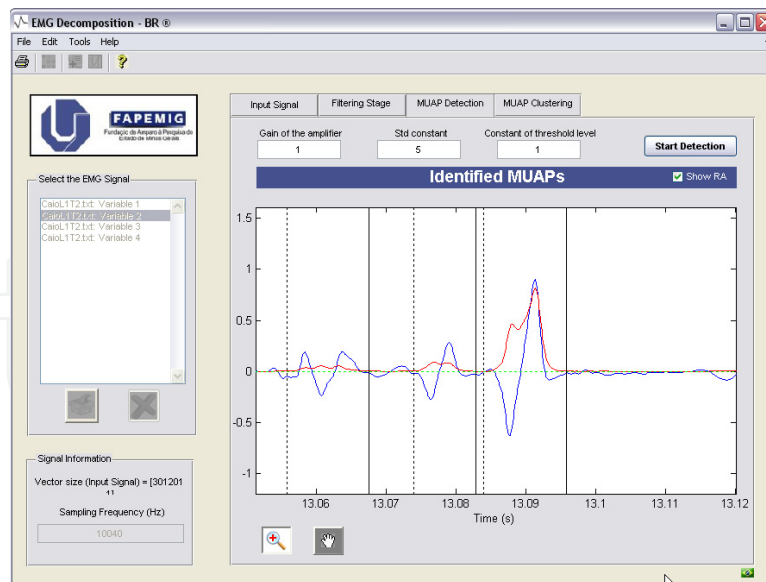
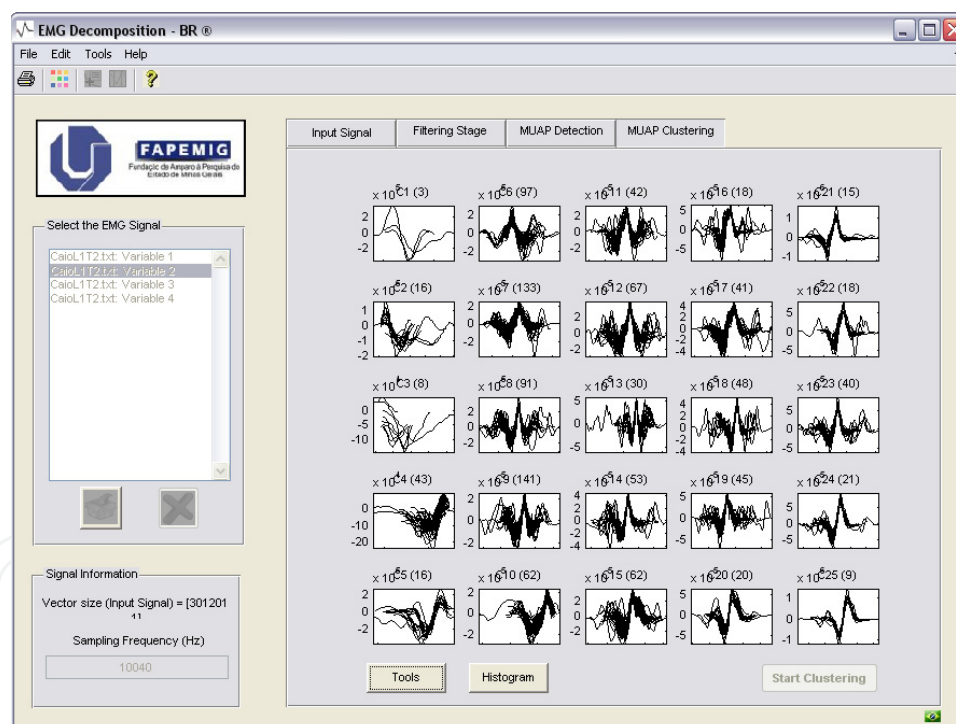**Figure 17.** Automatic detection of regions of activity.

Figure 18. Data clustering and visualization based on Generative Topographic Mapping [3, 9].

Hemiplegia and spasticity are among the most common post-stroke motor deficits. In general, hemiplegia is characterized by an initial flaccid stage, with motor and sensory losses, in which the patient finds himself unable to sustain or move the affected limb. In many cases, the motor sequel evolves into spasticity, a stage characterized by muscle hypertonia. Hemiplegia and spasticity are closely related to the disuse of the affected limb and to secondary changes in muscles, such as: selective atrophy of fast twitch type II muscle fibers, abnormal recruitment
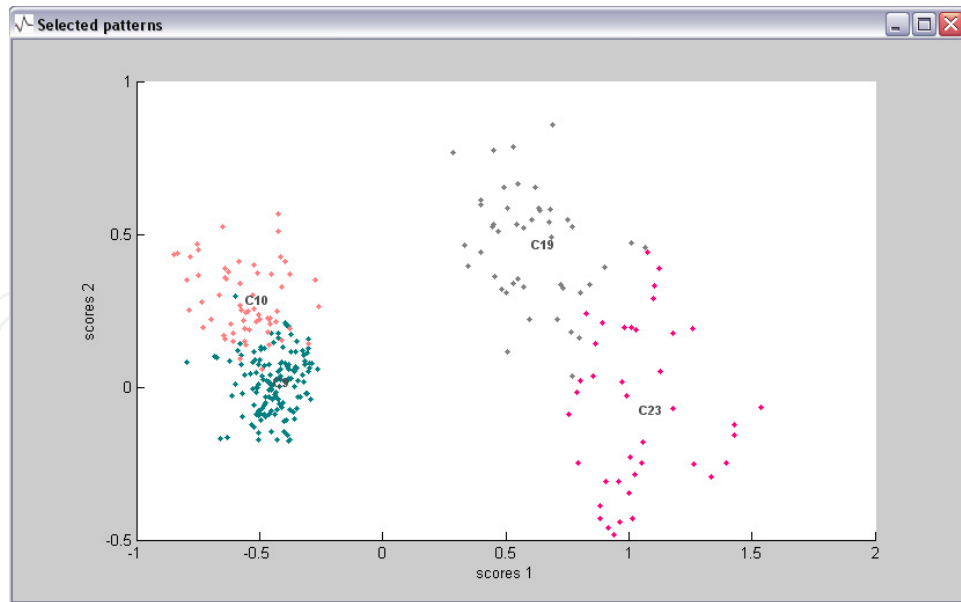
Figure 19. Two-dimensional visualization of groups of MUAPs obtained from the application of Principal Component Analysis.

of motor units, muscle contractures, and decreased cortical representation, due to disuse of the affected limb [28].

Several rehabilitation therapies have been used in an attempt to recover motor functionality, especially for upper limbs. The majority is based on the premise that the neural system can be retrained [20, 34]. The ability of the neural system to adapt to a new structural and functional condition, as well as its response to a traumatic destructive injury or to subtle changes resulting from the processes of learning and memory, is called 'neuroplasticity" [1, 12].

Recent studies have shown that behavioral experiments, important tools used in rehabilitation strategies based biofeedback techniques, have a strong impact on the motor cortical representation post-stroke. In this sense, we can also infer that it is possible to use biofeedback strategies for the modulation of neural plasticity, seeking the recovery of motor skills in rehabilitation protocols. The question is: how can we generate the appropriate information for feedback in a situation where the encephalic damage is manifested by an uncontrolled recruitment, or the lack of recruitment, of muscle fibers - leading to involuntary muscle hypotonia or hypertonia? Looking for a solution to this problem, a novel strategy, based in the assessment of the recruitment rate of motor units, is under test (see [39]), to generate control information for a multimodal biofeedback system. In this approach, instead of simply evaluating the process of muscle contraction, the researches decided to focus on the neural control over the muscles. However, the information regarding the recruitment of motor units are not readily available through standard surface EMG. Hence, the biofeedback relies heavily on a robust EMG decomposition system.

The strategy addressed by [39] is based on the discrimination and feature extraction of EMG signals (Motor Unit Action Potential) in order to control a virtual device. The biofeedback protocol immerses the patient in a virtual reality environment in which a representation of the affected limb will be presented. This virtual member is controlled according to the

pattern of motor unit recruitment. Thus, although the spastic or hemiplegic patient lacks of proper voluntary control, it is expected that the system will be able to capture small voluntary changes in motor recruitment, as a result of his desire to do so. These changes can then be used to guide the movements of the virtual member. In so doing, the virtual feedback operates as a guide, indicating that the current mental strategy (neuromotor control) is correct and should be encouraged, reinforcing the process of neural reorganization (neuroplasticity).

6. Future directions

The widespread use of automatic tools for decomposing EMG signals is dependent on how easy is to detect MUAPs from the surface of the skin, on the identification of new applications, either online or offline, which might employ the results of the EMG decomposition, and also on the sharing and availability of developed tools to clinicians and researchers.

Ideally the sensors used for detecting MUAPs from the surface of the skin should be easy of applying and using. As a number of applications require the use of multiple sensors organized on an array the solution to this issue becomes more complex. Therefore, further research on this area, with the aim of developing sensors that allow for the reproduction of experiments is required.

Most applications found in the area of EMG decomposition are solely focused on the development of the automatic tool for decomposing the EMG signal, or in the classification and discrimination of MUAPs. Therefore, the identification of new useful applications are required in order to disseminate the relevance of the technique to other areas. For instance, the use of motor unit information could be employed in robotics, myofeedback, and human-machine interface development.

A major limitation of the results in the area of EMG decomposition is that the developed tools are not shared by researchers. The sharing of these tools together with EMG signal databases could be beneficial to the widespread use of the tools. Furthermore, this would allow researchers to objectively compare distinct solutions.

Considering the application of artefact removal from biomedical signals, the development of algorithms for reducing the influence of noise over signals in real time, without a priori knowledge about the origins and characteristics of the noise, are required. In this way the application of adaptive techniques such as Empirical Mode Decomposition should be further exploited.

It is also expected that the use of these filters can be part of the solution of the problem of EMG decomposition by directly decomposing the raw EMG signal into its motor unit action potential trains. If such filters are developed, EMG decomposition tools could be embedded in hardware speeding up the results from multichannel data.

Acknowledgements

Author details

Adriano O. Andrade and Alcimar B. Soares
Faculty of Electrical Engineering, Laboratory of Biomedical Engineering, Federal University of Uberlândia, Uberlândia, Brazil

Slawomir J. Nasuto
School of Systems Engineering, University of Reading, Reading, United Kingdom

Peter J. Kyberd
Institute of Biomedical Engineering, University of New Brunswick, Fredericton, Canada

7. References

[1] I Adams. Comparison of synaptic changes in the precentral and postcentral cerebral cortex of aging humans: a quantitative ultrastructural study. *Neurobiology of Aging*, 8:203–12, 1987.

[2] Metin Akay. *Biomedical signal processing*. Academic Press, Inc, San Diego, California, 1st edition, 1994.

[3] Adriano O Andrade. *Decomposition and Analysis of Electromyographic Signals*. PhD thesis, University of Reading, Reading, UK, 2005.

[4] Adriano O Andrade, Peter J Kyberd, and Slawomir J Nasuto. Time-frequency analysis of surface electromyographic signals via Hilbert spectrum. In Serge H Roy, Paolo Bonato, and Jens Meyer, editors, *XVth ISEK Congress - An Invitation to Innovation*, page 68.

[5] Adriano O Andrade, Peter J Kyberd, and Slawomir J Nasuto. The application of the Hilbert spectrum to the analysis of electromyographic signals. *Information Sciences*, 178(9):2176–2193, 2008.

[6] Adriano O Andrade, Peter J Kyberd, and Sean D Taffler. A novel spectral representation of electromyographic signals. In Ron S. Leder, editor, *Engineering in Medicine and Biology Society - 25th Annual International Conference*, volume 1, pages 2598–2601. IEEE.

[7] Adriano O Andrade, Slawomir J Nasuto, and Peter J Kyberd. EMG signal filtering based on empirical mode decomposition. *Biomedical Signal Processing and Control*, 1(1):44–55, 2006.

[8] Adriano O Andrade, Slawomir J Nasuto, and Peter J Kyberd. Extraction of motor unit action potentials from electromyographic signals through generative topographic mapping. *Journal of the Franklin Institute*, 344(3-4 (May-July)):154–179, 2007.

[9] Adriano O Andrade, Slawomir J Nasuto, Peter J Kyberd, and Catherine M Sweeney-Reed. Generative topographic mapping applied to clustering and visualization of motor unit action potentials. *Biosystems*, 82(3):273–84, 2005.

[10] American Heart Association. Heart disease and stroke statistics — 2011 update: a report from the american heart association. *Circulation*, 123:e18–e209, 2011.

[11] Alfredo Avellido and Adriano O Andrade. Determination of feature relevance for the grouping of motor unit action potentials through a generative mixture model. *Biomedical Signal Processing and Control*, 2:111–121, 2007.

[12] S N Burke and C A Barnes. Neural plasticity in the ageing brain. *Nature Reviews Neuroscience*, (7):30–40, 2006.

[13] Lokenath Debnath and Piotr Mikusinski. *Introduction to Hilbert Spaces with applications*. Academic Press, San Diego, CA, second edition, 1999.

[14] David L Donoho. De-noising by soft-thresholding. *IEEE Transactions on Information Theory*, 41(3):613–627, 1995.

[15] H Etawil and Daniel W Stashuk. Resolving superimposed motor unit action potentials. *Medical and Biological Engineering and Computing*, 34(1):33–40, 1996.

[16] Jianjun Fang, Gyan C Agarwal, and Bhagwan T Shahani. Decomposition of multiunit electromyographic signals. *IEEE Transactions on Biomedical Engineering*, 46(6):685–697, 1999.

[17] Gonzalo A. Garcia, Kenzo Akazawa, and Ryuhei Okuno. Decomposition of surface electrode-array electromyogram of biceps brachii muscle in voluntary isometric contraction. In *Engineering in Medicine and Biology Society - 25th Annual International Conference*, pages 2483–2486. IEEE.

[18] Tamara Grujic and Ana Kuzmanic. Denoising of surface emg signals: a comparison of wavelet and classical digital filtering procedures. *Technology and Healthcare*, 12(2):130–135, 2004.

[19] Mohamed H Hassoun, Chuanming Wang, and A Robert Spitzer. NNERVE: Neural network extraction of repetitive vectors for electromyography - part I: Algorithm. *IEEE Transactions on Biomedical Engineering*, 41(11):1039 – 1051, 1994.

[20] Koichi Hiraoka. Rehabilitation effort to improve upper extremity function in post-stroke patients: A meta-analysis. *Journal of Physical Therapy Science*, 13:5–9, 2001.

[21] Norden E Huang, Zheng Shen, Steven R Long, Manli C Wu, Hsing H Shih, Quanan Zheng, Nai-Chyuan Yen, Chi Chao Tung, and Henry H Liu. The empirical mode decomposition and the Hilbert spectrum for nonlinear and non-stationary time series analysis. *Proceedings of Royal Society of London*, 454:903–995, 1998.

[22] R S LeFever and Carlo J De Luca. A procedure for decomposing the myoelectric signal into its constituent action potentials–part I: Technique, theory, and implementation. *IEEE Transactions on Biomedical Engineering*, 29(3):149–57, 1982.

[23] M. Lei and G. Meng. Classification of the action surface emg signals based on the dirichlet process mixtures method. volume 7101 LNAI of *4th International Conference on Intelligent Robotics and Applications, ICIRA 2011*, pages 212–220. Aachen, 2011.

[24] I Lessa. Epidemiologia das doenças cerebrovasculares no brasil. *Revista da Sociedade de Cardiologia do Estado de Sao Paulo*, 4:509–518, 1999.

[25] Michael S Lewicki. A review of methods for spike sorting: the detection and classification of neural action potentials. *Comput. Neural Syst.*, 9:R53 – R78, 1998.

[26] H Lohninger. *Teach/Me Data Analysis*. Springer-Verlag, Berlin, Germany, 1999.

[27] Carlos J De Luca. Decomposition of the EMG signal into constituent motor unit action potentials. *Muscle Nerve*, 18(12):1492–4, 1995.

[28] L Lundy-Ekman. *Neurociencias: fundamentos para reabilitaçao*, pages 155–199. Elsevier, Rio de Janeiro, 2008.

[29] Bruno Mambrito and Carlo J. De Luca. A technique for the detection, decomposition and analysis of the EMG signal. *Electroencephalography and clinical neurophysiology*, 58:175–188, 1984.

[30] H. R. Marateb, S. Muceli, K. C. McGill, R. Merletti, and D. Farina. Robust decomposition of single-channel intramuscular emg signals at low force levels. *Journal of Neural Engineering*, 8(6), 2011.

[31] N E Mayo, S Wood-Dauphinee, S Ahmed, C Gordon, J Higgins, S McEwen, and N Salbach. Disablement following stroke. *Disabil. Rehabil.*, 21(5-6):258–268, 1999.

[32] Kevin C. McGill, Kenneth L. Cummins, and Leslie J. Dorfman. Automatic decomposition of the clinical electromyogram. *IEEE Transactions on Biomedical Engineering*, BME-32(7):470–477, 1985.

[33] Michel Misiti, Yves Misiti, Georges Oppenheim, and Jean-Michel Poggi. *Wavelet toolbox user's guide*. The Mathworks, Inc, third edition, 2004.

[34] Susan O'Sullivan and Thomas Schmitz. *Fisioterapia: Avaliaçao e Tratamento*. Manole, 2010.

[35] H. Parsaei and D. W. Stashuk. A method for detecting and editing mupts contaminated by false classification errors during EMG signal decomposition. *33rd Annual International Conference of the IEEE Engineering in Medicine and Biology Society, EMBS 2011*, pages 4394–4397.

[36] H. Parsaei and D. W. Stashuk. SVM-based validation of motor unit potential trains extracted by EMG signal decomposition. *IEEE transactions on biomedical engineering*, 59(1):183–191, 2012.

[37] Constantinos S Pattichis and Marios S Pattichis. Time-scale analysis of motor unit action potentials. *IEEE Transactions on Biomedical Engineering*, 46(11):1320 – 1329, 1999.

[38] G. L. Sheean. Quantification of motor unit action potential energy. *Clinical Neurophysiology*, 123(3):621–625, 2012.

[39] M B Silva, D Viera, Ângela A R de Sá, and Alcimar Barbosa Soares. Proposta de treinamento com biofeedback eletromiográfico em ambiente de realidade virtual como apoio a reabilitaçao motora após acidente vascular encefálico. In *2o Congresso Brasileiro de Eletromiografia e Cinesiologia, COBEC 2012*, pages 1–3.

[40] Daniel W Stashuk. Decomposition and quantitative analysis of clinical electromyographic signals. *Med Eng Phys*, 21(6-7):389–404, 1999.

[41] Daniel W Stashuk and G M Paoli. Robust supervised classification of motor unit action potentials. *Medical and Biological Engineering and Computing*, 36:75–82, 1998.

[42] Daniel W Stashuk and Y Qu. Adaptive motor unit action potential clustering using shape and temporal information. *Medical and Biological Engineering and Computing*, 34(1):41–9, 1996.

[43] Tzyh-Yi Sun, Thy-Sheng Lin, and Jia-Jin Chen. Multielectrode surface EMG for noninvasive estimation of motor unit size. *Muscle and Nerve*, 22:1063 – 1070, 1999.

[44] S Usui and I Amidor. Digital low-pass differentiation for biological signal processing. *IEEE Transactions on Biomedical Engineering*, 29:686–693, 1982.

[45] N. W. Willigenburg, A. Daffertshofer, I. Kingma, and J. H. van Dieën. Removing ecg contamination from emg recordings: A comparison of ica-based and other filtering procedures. *Journal of electromyography and kinesiology*, 2012.

[46] Zhengquan Xu and Shaojun Xiao. Digital filter design for peak detection of surface EMG. *Journal of Electromyography and Kinesiology*, 10:275–281, 2000.

[47] F. Zaheer, S. H. Roy, and C. J. De Luca. Preferred sensor sites for surface emg signal decomposition. *Physiological Measurement*, 33(2):195–206, 2012.

[48] Daniel Zennaro, Peter Wellig, Volker M. Koch, George S. Moschytz, and Thomas Laubli. A software package for the decomposition of long-term multichannel EMG signals using wavelet coefficients. *IEEE Transactions on Biomedical Engineering*, 50(1):58–69, 2003.

[49] Ping Zhou, Zeynep Erim, and W Z Rymer. Motor unit action potential counts in surface electrode array EMG. In *Engineering in Medicine and Biology Society - 25th Annual International Conference*, pages 2067–2070. IEEE.